Cartographic displacement using the snakes concept

Article · January 1997

2 authors, including:

Dirk Burghardt
Technische Universität Dresden

Semanitic Modeling for the Acquisition of Topografic
Information from Images and Maps
ed. by W. Förstner and L. Plümer

Cartographic Displacement Using the Snakes Concept

Dirk Burghardt and Siegfried Meier

Department of Geosciences, Dresden University of Technology
e-mail: burg@ipg.geo.tu-dresden.de

Abstract

Symbolized images (maps) with a very high information density have to be generalized sometimes, i.e. objects have to be displaced reciprocally. A displacement algorithm which operates by the principle of the snakes concept is described. The addition of active splines, so-called snakes, to contours (attraction) is one possiblity to recognize indefinite contours. Another one is the reciprocal displacement of lines which is exactly the inversion (repulsion) of the previous method. Due to this equivalency the snakes technique may be also applied to line displacement. The described algorithm of energy minimization provides (carto)graphically sufficient solutions. Geometric and semantic control parameters take care to optical resolution, maintenance of topological structures, minimal changes in geometry and consider the object significance.

1 Introduction

In computer graphics and in cartography sometimes symbolized images with very high information density and insufficient visual resolution or graphic constraints have to be generalized. Before starting the selection, which always means a loss of information, one should try to displace the objects in a reciprocal way as far as enough space is available. Usually, displacement problems are of hybrid nature, because geometric, topological and semantic relations between the objects to be displaced have to be considered.

Previous displacement algorithms have been working with fundamental geometric means and are still very afflicted with the cartographic way of thinking oriented to special cases and scale transitions. One exception is the spring tension model (Bobrich 1996), where an optimal principle is applied to cartographic displacement. To obtain a certain consistency between automatic recognition and elimination of graphic constraints the snakes technique can be used alternatively. Active splines (*snakes*) are added to them in an energy minimizing way (attraction) for best recognition of indefinite contours. The reciprocal line displacement is exactly the inversion of this process (repulsion); see Figure 1.

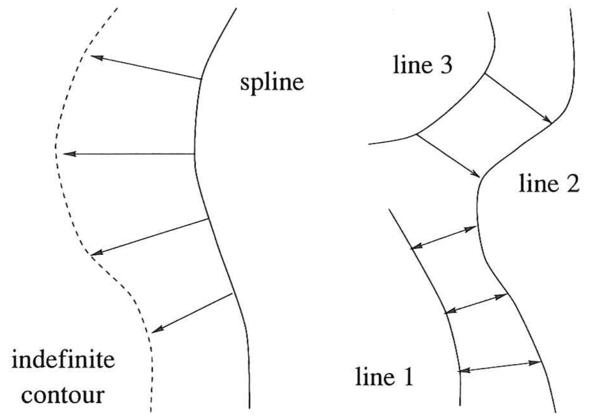

Fig. 1: Analogy between contour recognition (a spline is enclosed to an indefinite contour, left) and one-side or reciprocal line displacement (right) in the concept of energy-minimizing splines (snakes).

The equivalence of attractive and repulsive forces enables the application of the snakes technique by a variational problem also to displacement problems by minimizing the total energy. The numerical (iterative) solution algorithm, the so-called *greedy* algorithm (Williams and Shah 1990), or the stepwise solution of discretized *Eulerian* equations (Kass et al. 1987) can be used in the same way. Apart from this, the energies and potentials participating in the displacement problem should be formulated in a different way than in the recognition problem; see Table 1.

The displacement algorithm has been developed on the basis of the principle of energy minimization and tested within a first version. It provides (carto)graphically

	External Energy	Internal Energy
Recognition	Image Intensity	Direction and Curvature
Displacement	Displacement Potential	Differences in Directions Differences in Curvatures before and after Displacement

Tab. 1: Energies in the recognition and the displacement problem.

sufficient solutions. Geometric and semantic control parameters like hard-core distances which are to be given, displacement, direction and curvature potentials and weights according to object significance ensure the desired resolution. Furthermore, graphic constraints disappear whereas topological structures, fixed points and directions remain unchanged, position, direction and curvature of lines vary to a minimum extent. Finally, significant objects do not change their position, and insignificant objects are displaced.

2 Fundamentals of the Technique

2.1 The Principle of Energy Minimizing

The method of energy minimizing is applied among others to pattern recognition. It is known by the notion energy minimizing splines (snakes) (Kass et al. 1987) . In this article the method is adapted to line displacement. The question of the line course with the parameter representation $\mathbf{v} = [x(s), y(s)]^\top$ to minimize the functional

$$I(\mathbf{v}) := \int_0^1 E_{tot}\, ds = \int_0^1 (E_{ext} + E_{int})\, ds \qquad (1)$$

should be the initial point. The total energy E_{tot} is integrated along the line with the arc length s, $s \in [0,1]$. E_{tot} consists of internal and external energy. The external energy E_{ext} is used to describe the displacement cause. The short distances between the curve elements of different lines are decisive criteria. At the same time the original line shape which is described by its inclination and curvature are changed to a minimum extent. The above quantities are integrated in the internal energy E_{int}.

2.2 The Displacement Potential

The external energy E_{ext} is used to describe graphic constraints and amounts to zero if there are no displacement objects within a given minimum (hard-core) distance h from the place $\mathbf{v}_i = [x_i, y_i]^\top$. Point P_i represents an arbitrarily given point of the line L_I (see fig. 2). A displacement potential $E_{ext}(\mathbf{v}_i) > 0$ will develop in point P_i if the line or other displacement objects remain under the hard-core distance. The problem becomes more serious as the line segment extending within the hard core becomes longer and as the distance from P_i decreases. The simplest statement of the described requirements is

$$E_{ext}(\mathbf{v}_i) \sim \begin{cases} (1 - a/h) & : \; a < h \\ 0 & : \; a \geq h \end{cases} , \qquad (2)$$

where a is the distance between the line segment performing the displacement and the investigated point P_i for which the displacement potential is to be determined:

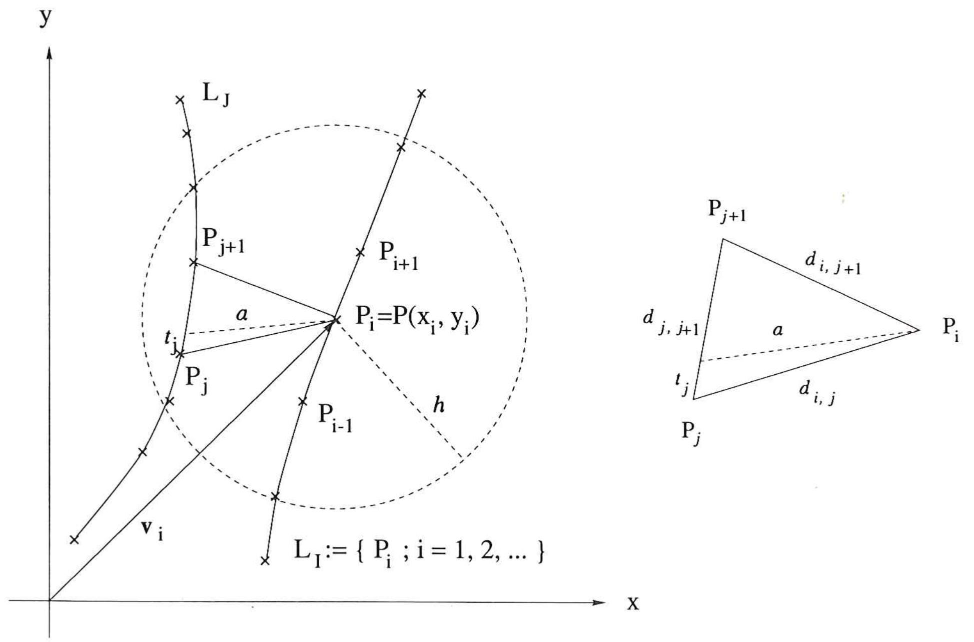

Fig. 2: Example of the determination of the displacement potential (in point P_i of the line L_I with respect to line L_J).

$$a = \sqrt{d^2_{j,j+1} \cdot t_j^2 + (d^2_{i,j+1} - d^2_{i,j} - d^2_{j,j+1}) \cdot t_j + d^2_{i,j}} \tag{3}$$

with

$$\begin{aligned} d_{j,j+1} &= \sqrt{(x_{j+1} - x_j)^2 + (y_{j+1} - y_j)^2} \quad , \\ d_{i,j} &= \sqrt{(x_j - x_i)^2 + (y_j - y_i)^2} \quad , \\ d_{i,j+1} &= \sqrt{(x_{j+1} - x_i)^2 + (y_{j+1} - y_i)^2} \end{aligned}$$

(cf. Appendix A1). The calculation is performed using the sliding average. The parameter t_j results from the ratio between the step size Δ and the individual distances of the given points:

$$t_j = \frac{\Delta}{d_{j,j+1}} \quad , \quad t_j \in [0,1) \quad . \tag{4}$$

The step size is given (fixed value) and can be chosen as an arbitrarily small value (at least one order of magnitude smaller than the average distance of the given values). Concerning $\Delta \to 0$ this corresponds to a quasi-continuous displacement.

2.3 The Shape Potential

The internal energy E_{int} is used to maintain the line shape which has been displaced due to conflicts. *Deviations* of first and second derivatives are used as quality measures (the sub-indices designate the partial derivatives by the arc length s):

$$E_{int} = (\alpha|w_s|^2 + \beta|w_{ss}|^2)/2 \tag{5}$$

with

$$\begin{aligned} w &:= (x - x^o, y - y^o) \quad , \\ w_s &:= (x_s - x_s^o, y_s - y_s^o) \quad , \\ w_{ss} &:= (x_{ss} - x_{ss}^o, y_{ss} - y_{ss}^o) \quad . \end{aligned}$$

In the iterative displacement process the differences in w_s and in w_{ss} always refer to the original line shape $(x^0, y^0, x_s^0, y_s^0, x_{ss}^0, y_{ss}^0)$. In general, term (5) agrees with the internal energy used in the snakes so far. The weights α and β are constant for each line (see Section 3.2).

3 Numerical Realization

3.1 Algorithms of Energy Minimization

The Variational Calculus. Let us regard a functional

$$I[x(s), y(s)] = \int_0^1 E_{tot}\, ds = \int_0^1 E_{tot}(x, x_s, x_{ss}, y, y_s, y_{ss}, s)\, ds \tag{6}$$

of two functions $x(s), y(s)$ with fixed boundary values

$$x(0) = x_a \quad , \quad y(0) = y_a \quad , \qquad x(1) = x_e \quad , \quad y(1) = y_e \quad .$$

The functions $x(s), y(s)$ with minimized functionals $I[x(s), y(s)]$ are wanted. An inevitable prerequisite is the stationarity of I in variation of the desired functions:

$$\delta I[x + \delta x, y] = 0 \quad , \quad \delta I[x, y + \delta y] = 0 \quad . \tag{7}$$

The Eulerian equations of the variational calculus for the two functions can be derived (Fliessbach 1992):

$$\begin{aligned} \delta I[x + \delta x, y] &= I[x + \delta x, y] - I[x, y] \\ &= \int_0^1 ds (E_x \delta x + E_{x_s} \delta x_s + E_{x_{ss}} \delta x_{ss}) \\ &= \int_0^1 ds (E_x - \frac{dE_{x_s}}{ds} + \frac{d^2 E_{x_{ss}}}{ds^2}) \delta x = 0 \quad . \end{aligned} \tag{8}$$

In this case $E_{x_{ss}} \delta x_{ss}$ develops to $(d^2 E_{x_{ss}}/ds^2)\delta x$ by partial integration done twice. The variation for the function $y(s)$ is performed in an analog way. Two differential equations of fourth order result from the arbitrariness of δx and δy, the Eulerian equations

$$E_x - \frac{dE_{x_s}}{ds} + \frac{d^2 E_{x_{ss}}}{ds^2} = 0 \ , \qquad E_y - \frac{dE_{y_s}}{ds} + \frac{d^2 E_{y_{ss}}}{ds^2} = 0 \ . \tag{9}$$

After the integration of the internal and external potential the following equations result:

$$\frac{\partial E_{ext}}{\partial x} - \alpha(x_{ss} - x^o_{ss}) + \beta(x_{ssss} - x^o_{ssss}) = 0 \ , \tag{10}$$

$$\frac{\partial E_{ext}}{\partial y} - \alpha(y_{ss} - y^o_{ss}) + \beta(y_{ssss} - y^o_{ssss}) = 0 \ . \tag{11}$$

The equations (10) and (11) are discretized by finite differences and are iteratively solved by Cholesky decomposition method (cf. Appendix A2).

The Greedy Algorithm. By the so-called greedy algorithm (Williams and Shah 1990) the energy minimization of lines can be easily performed. In this approach we attempt to reduce the energy *of each given value* by means of infinitesimal displacements. In the variational technique, however, the energy *of the whole line* is minimized in every iteration step. The transformation of conflict situations to the displacement potential (see paragraph 2.2) is the initial point of both techniques. The calculation of the internal energy is performed in a similar way. I.e. through the greedy algorithm the original line shape is registered by the explicite calculation of first and second derivatives on the given point positions :

$$E_{int} = E_{dis} + E_{curv} \tag{12}$$

with the following expressions:

$E_{dis} \sim \delta_0^2 - \delta_1^2$, while δ_0 is the original distance of the given points, δ_1 the distance of the given points after displacement,

and

$E_{curv} \sim \kappa_0^2 - \kappa_1^2$, while κ_0 is the orginal curvature, κ_1 the curvature after displacement.

E_{dis} is the energy part which results from differences in the first derivative between two iterations. These deviations can be geometrically interpreted as a change of the distance between the given points. In the analog way the contributions by variations in the second derivative are to be interpreted as curvature differences. The normalized distance between the given points results from

$$\delta = (\Delta x_i/\Delta s_i)^2 + (\Delta y_i/\Delta s_i)^2 \ , \qquad \Delta s_i^2 = \Delta x_i^2 + \Delta y_i^2 \ , \tag{13}$$

wherein $\Delta x_i = x_i - x_{i-1}$, $\Delta y_i = y_i - y_{i-1}$ are the coordinate differences between presently and previously given points. The curvature is calculated by

$$\kappa = (\Delta x_i/\Delta s_i - \Delta x_{i+1}/\Delta s_{i+1})^2 + (\Delta y_i/\Delta s_i - \Delta y_{i+1}/\Delta s_{i+1})^2 \ . \tag{14}$$

Concerning discrete calculation also the approach by Williams and Shah (1990) should be compared. Furthermore, we determine the direction in which the given points are to be displaced. For this an 8-neighbourhood with a step size that should be small in comparsion to the distances of the given points can be used. If the total energy of the given point is smaller at one point of the 8-neighbourhood, this point will be accepted as a new one (see Figure 3). Since the shape potential is created only by a change of the original position of the given points (which always means an energy increase), this increase has to be compensated by a reduction of the displacement potential.

In the first step the given points of all lines should be successively treated in this way. When all given points have a minimum of energy the iteration process will be concluded.

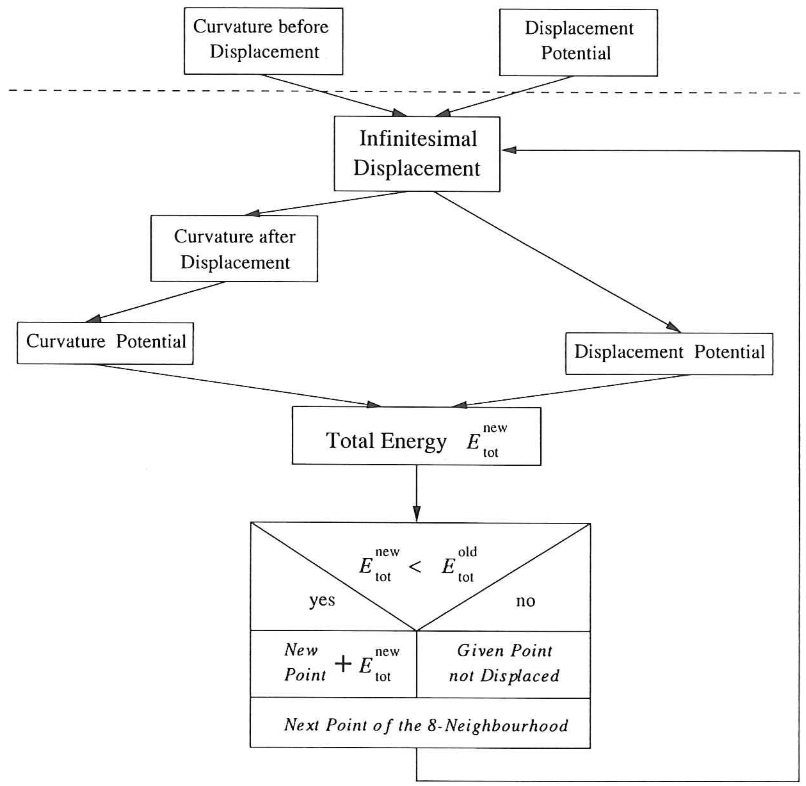

Fig. 3: Displacement scheme using the greedy algorithm.

3.2 Constraints and Controlling

Geometrical Constraints. The displacement potential is provided with a parameter to maintain the line shape around crossings. The above potential is a function of the distance between the lines, so that maximum values can be obtained in these areas. This means an orthogonalization of the (not neccessarily right-angled) crossing lines. On the one hand the mentioned parameter has to avoid the effect of orthogonalization and on the other hand a displacement of crossing lines by third objects must not be excluded. One possibility is to multiply the displacement potential by the factor

$$\chi^i(I,J) = \begin{cases} 1 & I \neq J \\ 0 & I = J \end{cases} \quad . \tag{15}$$

The superior index describes the given point for which the displacement potential has been calculated. The capital letters represent the lines.

At first the determination of the given points participated in line crossings is performed for the numerical calculation. If the conditions

$$D_1 D_2 < 0 \quad , \quad D_3 D_4 < 0 \quad \text{with} \tag{16}$$

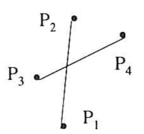

$$\begin{aligned} D_1 &= det(P_1, P_3, P_4) \ , \\ D_2 &= det(P_2, P_3, P_4) \ , \\ D_3 &= det(P_3, P_1, P_2) \ , \\ D_4 &= det(P_4, P_1, P_2) \ , \end{aligned} \qquad det(P_k, P_l, P_m) := \begin{vmatrix} x_k & x_l & x_m \\ y_k & y_l & y_m \\ 1 & 1 & 1 \end{vmatrix} ,$$

are fulfilled, the distances P_1P_2 , P_3P_4 will form a crossing and their intersection point will be fixed (Bartelme 1995). All given points P_i of the line I, situated within a given displacement depth can be marked now by the number of the involved line J. In this way an increase of the displacement potential of involved given points caused by crossing lines is excluded.

In the displacement patterns the topological relations are maintained by the procedure descrribed above. The displacement potential is defined in a way that an element can approach an adjacent one only up to the hard core, i.e. the adjacent element cannot be overjumped.

Semantic Controlling. In order to be able to control the displacement of the objects according to their significance weights are assigned. Objects of great significance and of high weight should be restrictively movable, while objects of less significance and of small weight should be more freely movable.

So far, we have only described how to change the *relative* position of objects. There are different possibilities to control the *absolute* position of lines:

i) The intensity of displacement is influenced. For that purpose the line is only partially integrated in the iterative displacement process or the step size is changed. Both procedures are controled by the significance of lines.

ii) Extension of the internal potential (5) by weighted term $\sim |w|^2$.

The first version is illustrated. According to their significance each object obtains a weight $p \in [p_{min}, p_{max}]$. In practical realization the iterative treatment of objects is used. As described earlier in Section 3.1 objects are displaced by small amounts. Before the execution of each iteration step it is decided by means of the weights, whether the object can be displaced. For a displacement the weights are interpreted as frequencies. By taking a random number z from the area of possible weights $(p_{min}, p_{max}]$ and by comparing it with the weight of the current object we can decide whether in this iteration step the object is to be displaced. The weighting of objects can be arbitrarily adapted to various applications. An object with p_{max} neither changes its position nor its shape.

Shape Controlling. The internal potential consists of two terms with the weights α and β (see Section 2.3). They control the evaluation of changed distances between given points and the deviations of line curvature during displacement. In simple cases the control for all line objects is performed with the same parameters. Larger weights provide lines with strong internal bonds.

In addition, parameters for the lines of different significance can be determined individually, the weights of the internal potential becoming semantic control parameters, too. Finally, we obtain the possibility to effect the curvature behaviour of parts of a line by using the parameters not as constants but as functions of the arc length: $\alpha = \alpha(s)$, $\beta = \beta(s)$.

3.3 Test Example

A typical conflict situation is illustrated by Figure 4(a): after transformation of the original image to a smaller scale line contacts and overlaps appear in the same symbol size. Line overlaps are displaced by energy minimization. Due to vector data (digitized line in figure 4(b)) the technique operates very fast.

As far as quality criteria are concerned the solutions from the variational technique (c) and the greedy algorithm (d) are both graphically admissible but deviate from each other, especially in the centre of the image and in the range of line crossings. The variational technique operates with fixed boundary values ("external constraint"), wherein the displacement process is stronger in the line centre than in the greedy algorithm. The mentioned effect is slightly reduced by the iterative solution of Eulerian equations. In the variational technique the typical line shape is maintained in a better way than in case of the greedy algorithm.

Sometimes the absolute position of "sharp curves" around line crossings is slightly changed. In the variational technique this applies to the upper crossing and in the greedy algorithm to the lower one. Until now these effects have not yet been eliminated and they should, with respect to the solution algorithm demonstrate, that the control parameters have to be carefully coordinated with each other (according to Section 3.2). In some cases a feed back mechanism or a trial-and-error technique should be used.

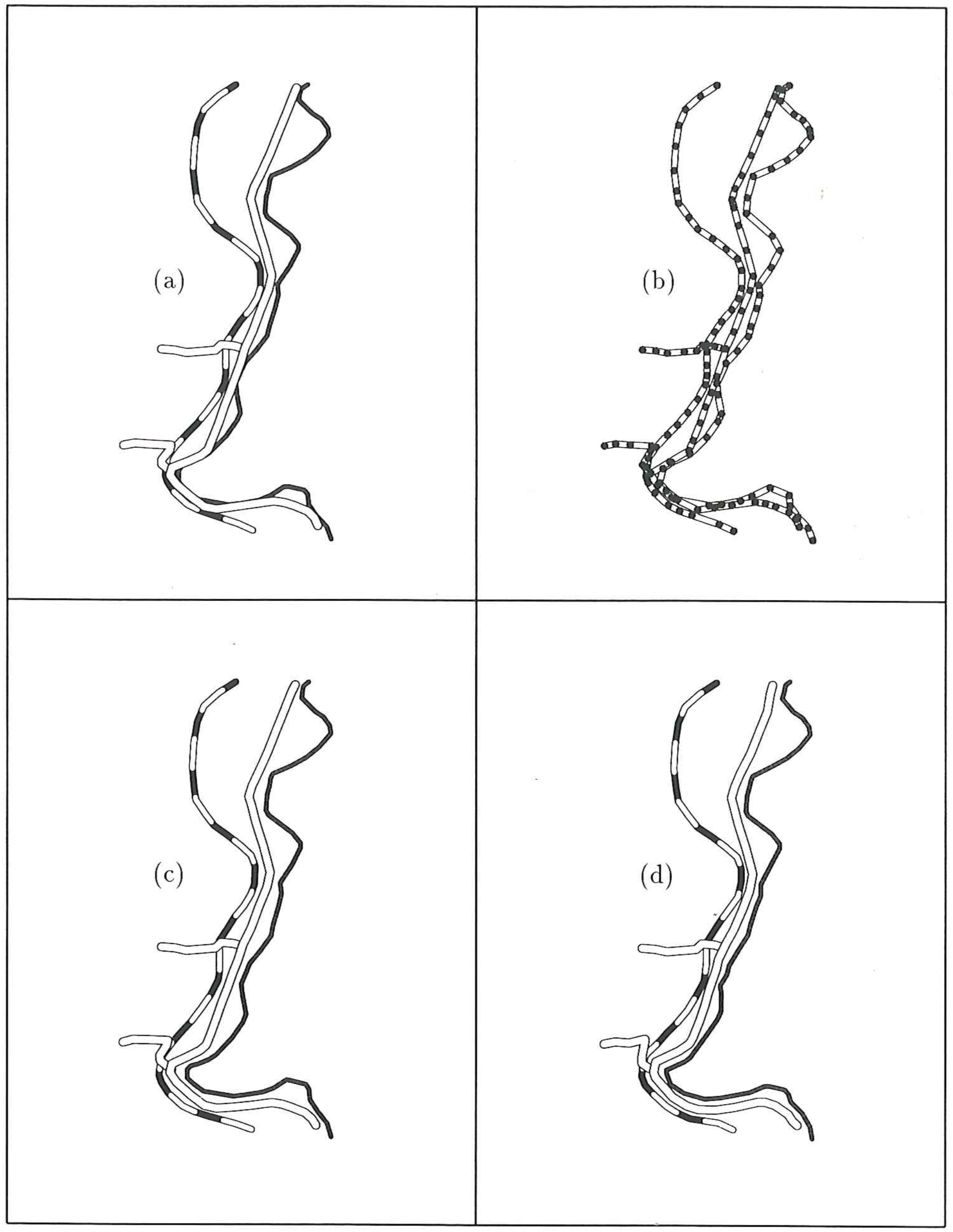

Fig. 4: Example of line displacement. Lines before displacement (a), digitized (b); after displacement by the variational technique (c) and the greedy algorithm (d).

4 Concluding Remarks

The above test example illustrates the application of the presented technique to line displacement. Point displacement by energy minimization is transformable in the same way. In the simplest case the parameters α and β of the internal potential are assumed to be zero, wherein all points are integrated in the displacement as isolated objects (point patterns). By this approach point and line displacements in mixed patterns are possible by means of the same algorithm.

So far in practical applications a linear displacement potential has been used. Other functional dependencies on the distance (quadratic progression, reciprocal distance model $1/r$) have been tested for simple examples without any visible effects. At the same time there exist different methods to calculate the curvature or the curvature potential from discrete data. They were investigated by Williams and Shah (1990) concerning their robustness.

Although the pilot version of the algorithm operates with suffcient results the problem of the adaption to practical tasks with various special cases, however, has still to be solved: definition of intersection according to data model and object structure, recognition and limitation of conflict situations, preferably by pattern recognition. The applications include large-scale and especially cadastral maps, topographic maps with coordinated scales and the transition to small scale general maps or the appertaining digital map models. Even the positioning of the lettering seems to be possible by energy minimization or by similar procedures.

Finally, we would like to underline the advantages of our computer-assisted displacement algorithm:

i) it is based on a generally valid subassigned principle, the energy minimization, therefore

ii) all special cases of graphical conflict situations in all possible data and object models, scale transitions, etc. can be solved, and

iii) it is consistent with the procedures of digital image processing.

Appendix A1:
Derivation of the distance a according to formula (3).

The starting point is the calculation of the distance between the points P_0 and P_i (Lang 1980).

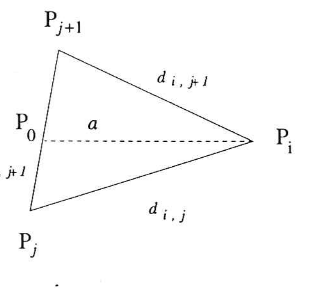

$$a^2 = (x_0 - x_i)^2 + (y_0 - y_i)^2 \tag{17}$$

P_0 moves from P_j to P_{j+1}:

$$x_0 = x_j + \Delta x \cdot t \ , \quad y_0 = y_j + \Delta y \cdot t \ , \tag{18}$$

wherein

$$\Delta x = x_{j+1} - x_j \ , \quad \Delta y = y_{j+1} - y_j \ .$$

The substitution of (18) in (17) leads to

$$\begin{aligned} a^2 &= (x_j - x_i + \Delta x \cdot t)^2 + (y_j - y_i + \Delta y \cdot t)^2 \\ &= (x_j - x_i)^2 + (\Delta x \cdot t)^2 + 2(x_j - x_i)(\Delta x \cdot t) \quad + \\ &\quad (y_j - y_i)^2 + (\Delta y \cdot t)^2 + 2(y_j - y_i)(\Delta y \cdot t) \\ &= d_{i,j}^2 + d_{j,j+1}^2 t^2 + 2t\,[(x_j - x_i)\Delta x + (y_j - y_i)\Delta y] \quad . \end{aligned} \tag{19}$$

With the boundary condition for $t = 1$ and $a = d_{i,j+1}$ in formula (19) we get

$$d_{i,j+1}^2 = d_{i,j}^2 + d_{j,j+1}^2 + 2\,[(x_j - x_i)\Delta x + (y_j - y_i)\Delta y] \quad . \tag{20}$$

Formula (3) results from the equations (19) and (20).

Appendix A2:
Discretization and solution of the Eulerian equations.

At first the equations (10) and (11) are discretized by the introduction of finite differences:

$$\begin{aligned} 0 = (E_x^i, E_y^i) &+ \alpha\,[(w_i - w_{i-1}) - (w_{i+1} - w_i)] \; + \\ \beta\,(\{[(w_i - w_{i-1}) &- (w_{i+1} - w_i)] - [(w_{i+1} - w_i) - (w_{i+2} - w_{i+1})]\} \; - \\ \{[(w_{i-1} - w_{i-2}) &- (w_i - w_{i-1})] - [(w_i - w_{i-1}) - (w_{i+1} - w_i)]\}) \quad . \end{aligned} \tag{21}$$

After conversion and with the substitutions

$$a := 2\alpha + 6\beta \qquad b := -\alpha - 4\beta \qquad c := \beta \tag{22}$$

the equation

$$0 = (E_x^i, E_y^i) + c w_{i-2} + b w_{i-1} + a w_i + b w_{i+1} + c w_{i+2} \tag{23}$$

results from (21), in matrix presentation

$$\mathbf{A}(\mathbf{x}^t - \mathbf{x}^0) = \mathbf{E_x}(\mathbf{x}, \mathbf{y}) \quad , \tag{24}$$
$$\mathbf{A}(\mathbf{y}^t - \mathbf{y}^0) = \mathbf{E_y}(\mathbf{x}, \mathbf{y}) \quad , \tag{25}$$

with the pentadiagonal band matrix

$$\mathbf{A} = \begin{pmatrix} a & b & c & 0 & 0 & \cdots \\ b & a & b & c & 0 & \\ c & b & a & b & c & \\ 0 & c & b & a & b & \\ 0 & 0 & e & d & a & \\ \vdots & & & & & \end{pmatrix} \quad . \tag{26}$$

In the next step the transition to an iterative treatment (parameter t) is performed:

$$(\mathbf{A} + \gamma\mathbf{I})(\mathbf{x}^t - \mathbf{x}^0) = \mathbf{x}^{t-1} - \mathbf{x}^0 - \mathbf{E_x}(\mathbf{x}^{t-1}, \mathbf{y}^{t-1}) \tag{27}$$
$$\underbrace{(\mathbf{A} + \gamma\mathbf{I})}_{\mathbf{B}}\underbrace{(\mathbf{y}^t - \mathbf{y}^0)}_{\mathbf{n}} = \underbrace{\mathbf{y}^{t-1} - \mathbf{y}^0 - \mathbf{E_y}(\mathbf{x}^{t-1}, \mathbf{y}^{t-1})}_{\mathbf{m}} \quad . \tag{28}$$

The vectors $\mathbf{x}^t$ and $\mathbf{y}^t$ represent the x- and y-coordinates of the line in the present iteration process. $\mathbf{x}^0$ and $\mathbf{y}^0$ are the x- and y-coordinates of the original line. The solution of the decoupled matrix equations (27) and (28) is realized by the Cholesky decomposition method. It is a symmetric version of the LR decomposition for positive definite matrices:

$$\begin{aligned} \mathbf{Bn} &= \mathbf{m} \\ \mathbf{R^T R n} &= \mathbf{m} \\ \mathbf{R^T u} &= \mathbf{m} \quad \Rightarrow \quad \mathbf{Rn} = \mathbf{u} \quad \Rightarrow \quad \mathbf{n} \quad . \end{aligned} \tag{29}$$

References

Bartelme N. (1995) *Geoinformatik - Modelle Strukturen Funktionen*, Springer-Verrlag, Berlin Heidelberg.

Bobrich J. (1996) *Ein neuer Ansatz zur kartographischen Verdrängung auf der Grundlage eines mechanischen Federkraftmodells*, Deutsche Geodätische Kommission, Reihe C, H. 455.

Fliessbach T. (1992) *Mechanik*, Wissenschaftsverlag, Mannheim, Leipzig, Wien, Zürich.

Kass M., A. Witkin, D. Terzopoulos (1987) *Snakes: Active contour models*, Proceedings of the First International Conference on Computer Vision, IEEE Comput. Soc. Press, pp. 259–268.

Lang W. (1980) *Gleitende Flächen mit strenger Berücksichtigung von Bruchkanten*, Master's thesis, Univ. Bonn.

Williams D. J., M. Shah (1990) *A fast algorithm for active contours and curvature estimation*, Proceedings of the Third International Conference on Computer Vision, IEEE Comput. Soc. Press, pp. 592–595.

Acknowledgement

The authors, who have not yet been involved in image processing so far, owe *Wolfgang Förstner* (Bonn) a debt of gratitude, because has drawn our attention to the excellent possiblities offered by the snakes technique. We also thank *Frank Bethge* (Dresden) who has assisted in our work in a critical and helpful manner.